Ph.D. Program in Civil, Chemical and Environmental Engineering
Curriculum in Fluid Dynamics and Environmental Engineering

Department of Civil, Chemical and Environmental Engineering
Polytechnic School, University of Genoa, Italy.

New Methodologies For The Characterization Of Extreme Sea States: Applications in the Mediterranean Sea

Francesco De Leo

New Methodologies For The Characterization Of Extreme Sea States: Applications in the Mediterranean Sea

BY

Francesco De Leo

Dissertation discussed in partial fulfillment of

the requirements for the Degree of

DOCTOR OF PHILOSOPHY

Civil, Chemical and Environmental Engineering

curriculum in Fluid Dynamics and Environmental Engineering,

Department of Civil, Chemical and Environmental Engineering, University of Genoa, Italy

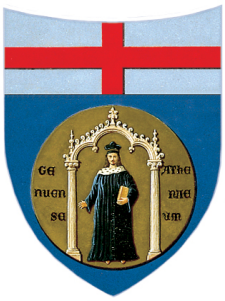

December, 2019

Adviser(s):
Prof. Giovanni Besio - Department of Civil, Chemical and Environmental Engineering, University of Genoa, Italy
Prof. Sebastián Solari - Insituto de Mecánica de los Fluidos e Ingeniería Ambiental, Universidad de la República de Uruguay, Uruguay

External Reviewers:
Prof. Miguel Ortega-Sánchez - School of Civil Engineering, University of Granada, Granada, Spain
Dr. Mark Hemer - Commonwealth Scientific and Industrial Research Organization, Australia

Examination Committee:
Prof. Alessandro Bottaro - Department of Civil, Chemical and Environmental Engineering, Uiversity of Genoa
Prof. Giorgio Bellotti - Department of Engineering, University of Roma Tre
Prof. Daniele Rocchi - Department of Mechanical Engineering, Polytechnic University of Milan

Ph.D. program in Civil, Chemical and Environmental Engineering
Curriculum in Fluid Dynamics and Environmental Engineering
Cycle XXXII

ABSTRACT

The sampling of met-ocean variables is crucial for a plethora of applications. In coastal areas, the management of coastal activities and shipping lanes have to account for variations on mean sea level, wave parameters and current velocities, and coastal defences need to be designed according to the severe sea states they will most likely have to face. Similarly, off-shore engineering projects are expected to stand against forces driven by waves that might occur, e.g., once in ten thousand years. The assessment of design waves relies on statistical extrapolations that need to be fed with reliable and continuous wave data. Therefore, it would be appropriate to extend as much as possible the possible ways of sampling waves. In this regard, this thesis first addresses the reliability of HF-radar wave measures, through a practical case study in the Gulf of Naples. Radar data are compared to the outcomes of two numerical models: one providing the wave parameters on a regional scale, and the other specifically developed for the area of investigation over finer resolutions. Both the models are previously validated against a buoy installed offshore the gulf (taken as reference), which is placed outside the radar domain and therefore cannot be employed for a direct comparison with the latter. The agreement between the models and the HF-radars is evaluated through error indexes computed on the significant wave heights, mean period and mean incoming directions. Results show a reasonable consistency between HF-radar and models measures, leaving room for further investigations on the use of such devices.

The aforementioned study refers to hindcast data provided by the Department of Civil, Chemical and Environmental Engineering of the University of Genoa (Italy). The hindcast was developed through a third generation wave model defined over the whole Mediterranean Sea, outputting the most significant wave parameters on a hourly base in the 1979-2018 period. Such data, being continuously defined over a long period, allow also to perform reliable analysis of the extreme waves for given locations. In particular, beyond the analysis of HF-radar wave measurements, this thesis proposes two insights in the framework of the so-called extreme value analysis (EVA).

First, a "bottom-up" approach for the identification and classification of the atmospheric processes producing extreme wave conditions is revisited, and applied to several locations selected among the Italian buoy network. A methodology is given for classifying samples of significant wave height peaks in homogeneous subsets, related to the climatic forcing driving the most severe wave states. Subsequently, the study shows how to compute the overall extreme values distribution of significant wave height starting from the distributions fitted to each single subset previously detected. From the obtained results, it is concluded that the proposed methodology is capable of identifying clearly differentiated subsets, driven by homogeneous atmospheric processes: two well-known cyclonic systems are identified as most likely responsible of the extreme conditions detected in the investigated locations. These systems are analyzed in the context of the Mediterranean Sea atmospheric climatology, and compared with those figured out by previous researches developed in similar frameworks. Then, it is proved that the high return period quantiles for the significant wave height are consistent with those resulting from the usual computational scheme of the EVA.

Finally, a simple model for evaluating non-stationarity in extreme waves is discussed, and possible implications are analyzed through practical examples. This model takes advantage of a linear slope estimate that allows to quantify the rate of change of a given time series of

data, lowering the weight of possible outliers. The reliability of this slope is proved against two other methods that are not bounded by the linear trend hypothesis, which in fact could represent a too limiting assumption. This study is applied to series of significant wave height annual statistics over the whole Mediterranean Sea. Trend tests are applied on the series carried out from the hindcast locations, and show that the modified linear slope is sound and reliable. Hence, it is shown how such index can be employed to evaluate for the need of non-stationary EVA rather than the common stationary ones, i.e. when significant divergences between the two models may arise. Finally, the linear slope estimates are used to assess the spatial distribution of historical long-term trend in the Mediterranean Sea, showing interesting analogies with previous works defined over similar locations.

INDEX

List of Figures

List of Tables

INTRODUCTION

The characterization of waves in seas and oceans is of primary importance in several fields of investigation. As an instance, waves are one of the most promising renewable energy sources, whose consumption is expected to rise considerably over the next decades, placing this source among the major carbon-free ones in many countries (Clément et al., 2002; Iglesias et al., 2009; Ferrari et al., 2019). Wave energy production can take place both off-shore, with floating devices that take advantage of the vertical motion of the sea surface (Henderson, 2006), and onshore; in the latter case, it is converted the energy carried by the waves when impacting the shore (Contestabile et al., 2016; Centurioni et al., 2017). Actually, as regards the coastal zones, the need of investigating the sea surface is manifold. Indeed, waves directly affect the variation of coastline profiles (Hanson, 1989). Driving the sediment dynamics in coastal regions, sea waves in turn influence the evolution of beach faces (Kraus et al., 1991). For example, seasonal variations in the average wave climate intensity, result on different equilibrium profiles for the cross-sections of a shore between winter and summer months, inducing periodic cycles of accretion and erosion of the emerged beach (see the left panel of Figure 1.2). In addition to that, intense storms impacting to the coast may lead to considerable retreats of a shoreline (Davis, 2012; Sherwood et al., 2014, an example is reported in the right panel of Figure 1.2). Information on wave characteristics are therefore needed for being able to get an insight on the coastal morphodynamic, which allows a proper planning of coastal land-use in the long term (Cicin-Sain, 1993). On the other hand, real-time monitoring and forecast of sea waves are crucial to predict hazardous conditions on coastal areas, providing decision-makers with prompt tools useful to manage the activities along the seaside.

Figure 1.1: Devices for wave energy conversion. Left panel: example of technology that uses the motion of ocean surface waves to create electricity (www.emec.org.uk); right panel: energy is produced by waves overtopping on a breakwater (www.conisma.it)

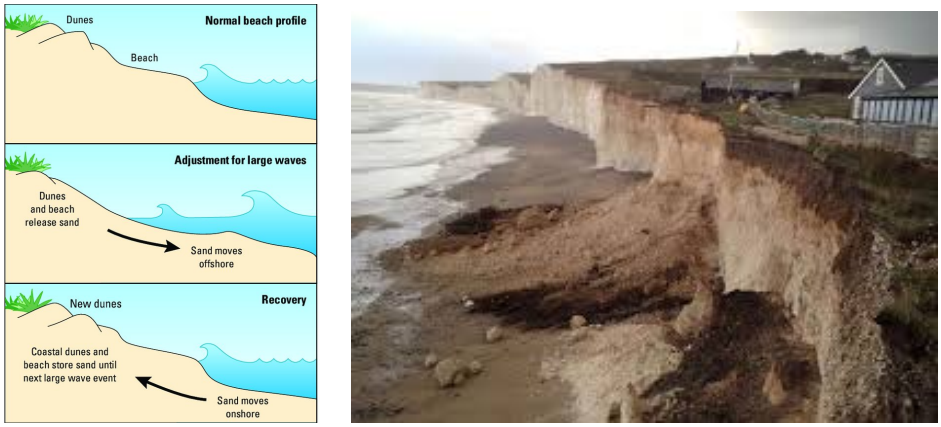

Figure 1.2: Left panel: example of seasonal variations of a beach face (Fletcher et al., 2012); right panel: storms-induced erosion of a cliff in UK (www.independent.co.uk)

Furthermore, the knowledge of sea conditions represents a key input for another relevant area, such as the maritime trade. In the past years cargo shipping has been one of the fastest growing economic sectors (Grossmann et al., 2007), and the United Nations Conference on Trade and Development is projecting a 3.4% growth in the world maritime trade for the period 20192024 (www.unctad.org). Needless to say, the optimization of shipping lanes and harbour operability, need to be tackled by especially considering the state of the sea surface (Bressan and Tinti, 2016).

As for the design of coastal defences (e.g. seawalls or rubble-mound breakwaters) and off-shore platforms, it is particularly relevant to characterize the condition of extreme waves (Pullen et al., 2007). Structures in the sea need to stand against forces driven by waves that are more extremes than any that might have been previously observed (Kottegoda and Rosso, 1997). This is aimed at minimizing the failure probability for maritime projects, as such an event would be extremely dangerous. The computation of design waves require to refer to statistical models, that allow to extrapolate the parameters of extreme waves beyond those sampled or modelled at a given location. These models do not depend upon the physical laws that rule the behavior of geophysical quantities, as such, they are often characterized by a huge uncertainty. Nevertheless, the availability of highly-populated and continuous wave datasets helps to reduce this uncertainty, leading to a better characterization and forecasting of unusually intense sea states.

The computation of design waves through statistical approaches belong to the branch of the so called Extreme Value Theory ("EVT"): this thesis introduces new methodologies in such framework. First, a new methodology for performing extreme waves based on Weather Patterns classification is introduced. Second, it is investigated how to properly detect trends in time series of data in order to evaluate the need of employing non-stationary models for the computation of design waves. These researches are shown in Chapter 4 and Chapter 5, respectively.

Figure 1.3: Examples of extreme waves impacting on maritime structures. Left panel: wave overtopping over a breakwater (www.ilmeteo.it); right panel: off-shore platform for oil & gas extraction (www.theamericanenergynews.com)

The examples so far introduced, highlight some of the applications for which it is essential to dispose of real-time wave data and/or historical records of wave fields at given locations. Therefore, it is worth to mention some of the most diffused methods among the surface gravity wave measurements.

The instrument that best catches the three dimensional motion of the sea surface is obviously the floating buoy (Figure 1.4 a)). This instrument is equipped with an accelerometer able to measure its vertical and horizontal motion, and radio communication to send their signals to land-based receiving stations (Krogstad et al., 1999). Among the *in-situ* techniques, there are also instruments usually fixed to the sea bottom, which measures the waves characteristics through up-looking beams that are reflected by the sea surface and/or suspended material (Van Haren, 2001); Figure 1.4 c) shows the example of an Acoustic Doppler Current Profiler. On the other hand, remote sensing techniques are mainly represented by satellite data, which receive reflections of the sea surface on the infra-red part of the light spectrum (Hwang et al., 2000), and HF-radars, which obtain the measurements from time-averaged power spectrum of the backscattered emitted signal (Wyatt et al., 2011). Examples of remote sensing techniques can be appreciated in Figure 1.4, panels c) and d).

Among the aforementioned instruments, HF-radars represent a challenging opportunity since they allow to take measures of both velocity currents and wave parameters. Other strengths of HF-radars are that they are installed on the ground, thus they are easy to access, and that they allow to collect information on wide portions of the surface, while e.g. buoys can only provide punctual information. Nonetheless, the use of radars for wave measurements present some drawbacks for which their use is still not diffused and precise and need to be further investigated. In view of the above, a case study on the analysis of radar-induced wave measures is reported in Chapter 3.

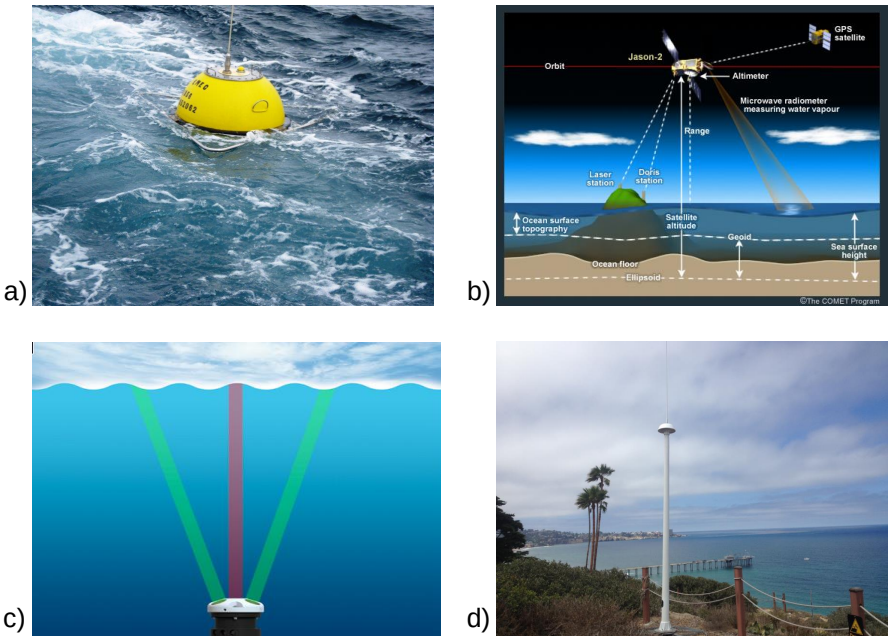

Figure 1.4: Devices for sampling the elevation of sea free surface. Panel a) waverider buoy at sea (source: www.emec.org.uk); panel b): sketch of data taken by a satellite (source: www.eumetsat); panel c) bottom-fixed ADCP (souce: www.sedexp.net); panel d): HF-radar (www.ioos.noaa.gov)

1.1. Outline of the thesis

The core of this thesis can be broken down into four main parts as follows.

Chapter 2

This Chapter introduces the basic theory of the sea waves. It first recalls the main parameters characterizing a wave. Then, it shows the methodologies for computing the wave characteristics of a sea state from the record of the surface oscillations. First, the up-crossing and down-crossing methods for the statistical description of sea states are introduced, then the spectral analysis is deepened. At a second time, a brief review of the types of extreme waves is presented. Finally, the models belonging to the Extreme Value Theory are explained and related to the applications explained further on the text.

Chapter 3

This Chapter shows a comparison between numerical models and HF-radar wave measurements. A case study in the Gulf of Naples is presented. This study takes advantage of two models defined at different spatial scales: one providing wave data on a regional scale, while the other is specifically set on the local area of investigation, and is defined over finer resolutions. Both the models are validated against data of a buoy placed just outside the gulf, and are

therefore taken as references in order to test the reliability of HF-radars measurements inside the gulf.

Chapter 4

This Chapter presents the study on the extreme wave height classification according to the weather patterns they most likely belong to. The methodology proposed is applied to eight hindcast locations along the Italian coastline, characterized by different wave climates. A clustering technique is employed to classify extreme wave heights in different clusters, according to the wind fields directly affecting the wave climate at the selected locations. At a second time, a Monte Carlo scheme is suggested for the development of long return period wave heights starting from the models fitted to each subset.

Chapter 5

This Chapter reports a critical review on the use of linear slope estimates for the detection of climate trends in wave height series. Three different models for trend analysis are applied to annual statistics of wave hindcast data in the Mediterranean Sea. The outcomes of the models are compared in order to evaluate their consistency. At a second time, trend tests are evaluated in relation to the non-stationary Extreme Value Analysis, and finally the spatial distribution of trends in the Mediterranean Sea is analyzed.

STATE OF THE ART

2.1. Waves in sea and ocean

According to the Encyclopaedia Britannica, a wave is a propagation of disturbances from place to place in a regular and organized way. This implies a periodic change from the equilibrium profile of a certain field: in case of sea waves, this field is the sea surface.

Figure 2.1 reports a sketch of a wave, showing as well the parameters that characterize it; these parameters as summarized as follows:

- A_c is the wave amplitude. It indicates the vertical distance between a crest or a trough and the equilibrium profile, the latter being represented by the black horizontal line;
- H is the wave height, defined as the total distance between the crest and the trough. For monochromatic waves, H is twice A_c;
- T is the wave period. It is the time elapsed between the passage of two successive points at the same elevation. In this case, the x-axis in the sketch refers to time;
- L is the wavelength. It is the distance over which the wave's shape repeats. In this case, the x-axis in the sketch refers to space.

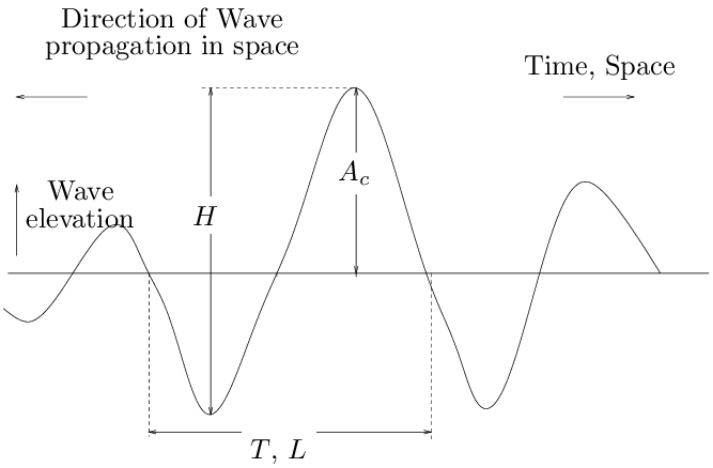

Figure 2.1: Parameters of a wave (Brodtkorb, 2004)

As regards the sea waves, they can be thought as vertical motion of the ocean surface (Holthuijsen, 2010); such waves can be ordered due their lengths and periods, as shown in Figure 2.2 (Munk, 1949).

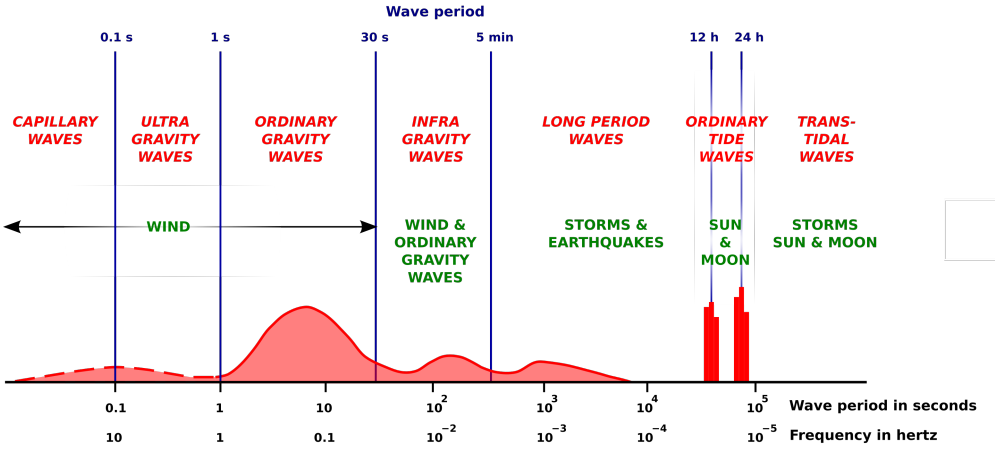

Figure 2.2: Frequencies and periods of different waves in the ocean environment

From now on, the text will refer to ordinary gravity waves, whose periods range in the 1-30 s interval. This class of waves embeds two different wave systems, i.e. *wind waves* and *swells*. The former are driven by the wind blowing over the sea surface and transferring energy to the water body; these waves are characterized by a huge randomness and are most likely to be observed in their area of generation. The latter are waves no longer affected by wind; indeed, they can travel over long times and distances, and they might have been generated very far from where they are observed. These waves are characterized by a more regular shape (Komar, 1998). Examples of these systems can be appreciated in Figure 2.3.

By looking at the examples it appears clear how the sea waves are characterized by more complex and chaotic shapes than that of Figure 2.1 (especially in case of wind waves). Therefore, sea states are always defined according to average parameters, that summarize the information of sea states taking place over certain intervals of time. The averaging of the sea surface should be performed over sea states characterized by statistical stationarity, which at sea implies to refer to time frames of 15-30 minutes (Holthuijsen, 2010). In such an interval, from the records of the mean water level elevation it is possible to describe the mean sea state parameters via two different approaches: a statistical description of sea waves, and/or a spectral analysis. Both the approaches are following introduced.

Figure 2.3: Different types of waves. Left panel: wind waves in the deep water; right panel: swell approaching the shore

2.1.1. Statistical short-term description of sea waves

Suppose to have a time record of surface elevation such that of Figure 2.4; surface elevation is defined as the instantaneous elevation of sea surface with respect to a reference level (e.g. the mean sea level). From now on, surface elevation will be referred to as η. In such a record, a single wave can be identified in two different ways: i) as the profile embedded between two successive points where η passes from negative to positive values (underlined with the red letter u in Figure 2.4); ii) as the profile embedded between two successive points where η passes from positive to negative values (underlined with the red letter d in Figure 2.4). The first and the latter approaches are called *up-crossing* and *down-crossing* method, respectively.

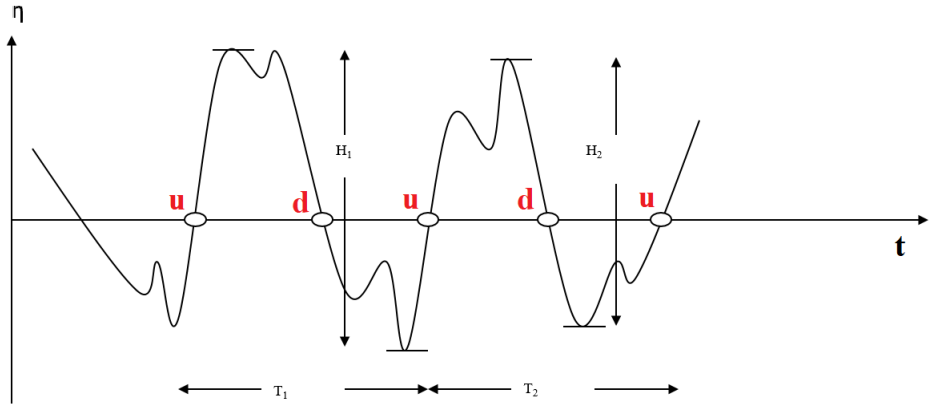

Figure 2.4: Sketch for the up-crossing and down-crossing methods; the points used as reference for defining the single waves are highlighted with red letters

Once a wave has been defined, it is possible to assign the respective height H, defined as the vertical distance between the highest and the lowest elevation of η between either two successive up-ward or down-ward zero crossing points. Accordingly, the horizontal distance between such pairs of points defined the period T of the single wave.

Given a series of $H_{1:N}$ data, after the sample has been sorted in increasing order, the following parameters, related to a certain time frame, can be computed:

- mean wave height: $\bar{H} = \frac{1}{N}\sum_{i=1}^{N} H_i$
- root mean-square wave height: $H_{rms} = \sqrt{\frac{1}{N}\sum_{i=1}^{N} H_i^2}$
- significant wave height: $H_{1/3} = \frac{1}{N/3}\sum_{i=2/3N}^{N} H_i$
- one-tenth wave height: $H_{1/10} = \frac{1}{N/10}\sum_{i=9/10N}^{N} H_i$

The significant wave height, most often referred to as H_s, is close to the wave that can be visually observed in a sea state, and it is therefore the most used statistic in met-ocean applications.

The relations between the different statistics is summarized in Figure 2.5, reporting the probability density function of a Rayleigh distribution:

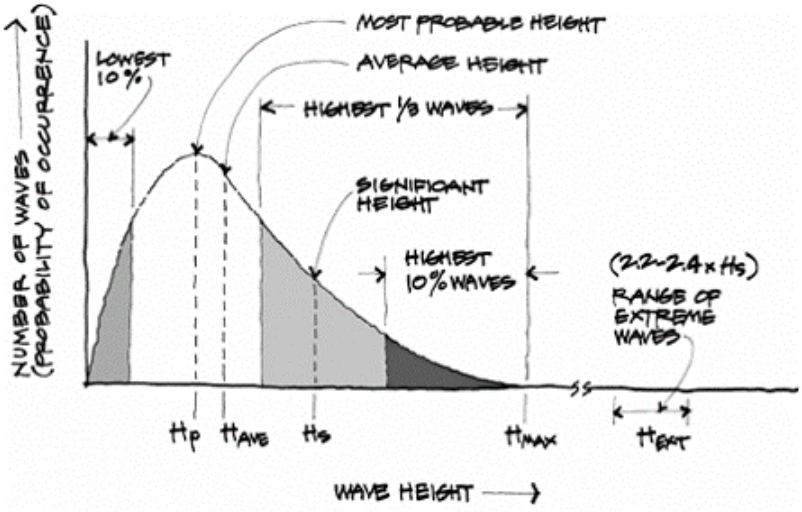

Figure 2.5: Rayleigh distribution for zero-crossing wave heights

This distribution is usually employed to describe the up-crossing and/or down-crossing wave heights, and its density function is expressed as:

$$p(H;\sigma) = \frac{H}{\sigma_R^2} \exp\left(-\frac{H^2}{2\sigma_R^2}\right) \tag{2.1}$$

where σ_R is the parameter of the distribution.

The statistics of the wave period are defined relatively to H, i.e. they are computed according to the subsets of waves sorted due to their height (with the exception of the mean period):

- mean period: $\bar{T} = \frac{1}{N}\sum_{i=1}^{N} T_i$
- significant wave height: $T_{1/3} = \frac{1}{N/3}\sum_{i=2/3N}^{N} T_i$
- one-tenth wave height: $T_{1/10} = \frac{1}{N/10}\sum_{i=9/10N}^{N} T_i$

It is evident that through the statistical description of the sea states only few parameters can be defined, since is not possible to fully characterize the randomness of a sea state. To this end, the surface elevation has to be modeled as a stochastic process, and therefore defined in terms of the so-called *wave spectrum*.

2.1.2. The wave spectrum

The wave spectrum theory assumes that the surface of the sea can be seen as the superimposition of an infinite number of waves, characterized by their own frequencies and directions. Anyhow, for the sake of clarity, suppose at first sight that the system is characterized by waves propagating along a single direction. Under this assumption, the record of surface elevation can be seen as the sum of a large number of harmonics wave components (a Fourier series, Holthuijsen, 2010)

$$\eta(t) = \sum_{i=1}^{N} A_{c_i} \cos(2\pi f_i t + \phi_i) \tag{2.2}$$

where A_{c_i} and ϕ_i are the amplitude and phase, respectively, of the i^{th} frequency.

Hence, the wave spectrum is the distribution of the energy of the single waves against the respective frequencies. A simple example, related to few sinusoidal components, can be appreciated in Figure 2.6: in case of sea waves, the frequency distribution is no longer represented by single bins, but through a regular curve that catches the ideally infinite number of single components. This curve can be expressed via parametric distributions, such as the JONSWAP spectrum (Hasselmann et al., 1973) or the Pierson-Moskowitz spectrum (Pierson and Moskowitz, 1964), among other models. These functions express the density $S(f)$, defined as $a^2/(2f)$, as a function of f. The JONSWAP model will be recalled further on the text (see Chapter 3), therefore is here introduced:

$$\begin{cases} S(f) = \dfrac{\alpha g^2}{f^5} \exp\left[\dfrac{5}{4}\left(\dfrac{f_p}{f}\right)^4 \gamma^r\right] \\ r = \exp\left[-\dfrac{(f-f_p)^2}{2\sigma^2 f_p^2}\right] \\ \alpha = 0.076 \left(\dfrac{U_{10}^2}{Fg}\right)^{0.22} \\ f_p = 22 \left(\dfrac{g^2}{U_{10} F}\right)^{1/3} \end{cases} \tag{2.3}$$

where f_p is the peak frequency, U_{10} is the wind speed at a height of 10 m above the sea surface, F is the distance from a lee shore (the fetch), g is the gravity force, σ is equal to 0.07 (0.09) if $f \leq f_p$ ($f > f_p$), γ is the peak enhancement parameter. An example of the JONSWAP spectrum is shown in Figure 2.7.

Once $S(f)$ is known, the spectral moments ca be defined:

$$m_r = \int_{f_l}^{f_u} f^r S(f) df \tag{2.4}$$

being f_l and f_u the lower and upper cut-off frequencies of the spectrum, respectively.

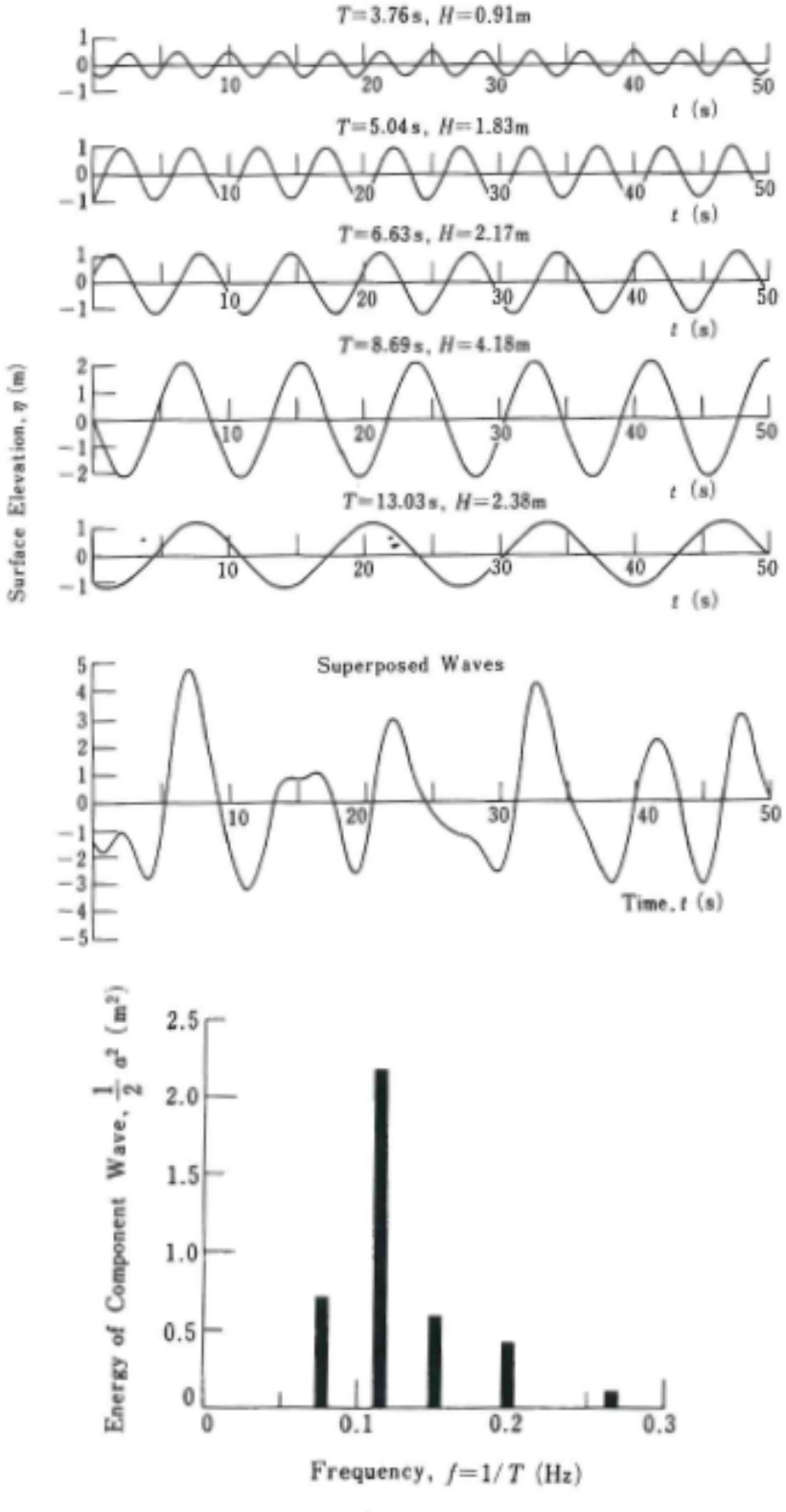

Figure 2.6: Example of a spectral description of a sea state. Upper panel: simulation of irregular waves by superposition of sinusoidal waves; lower panel: spectral representaion of superposed waves. This example is taken from Goda (1988)

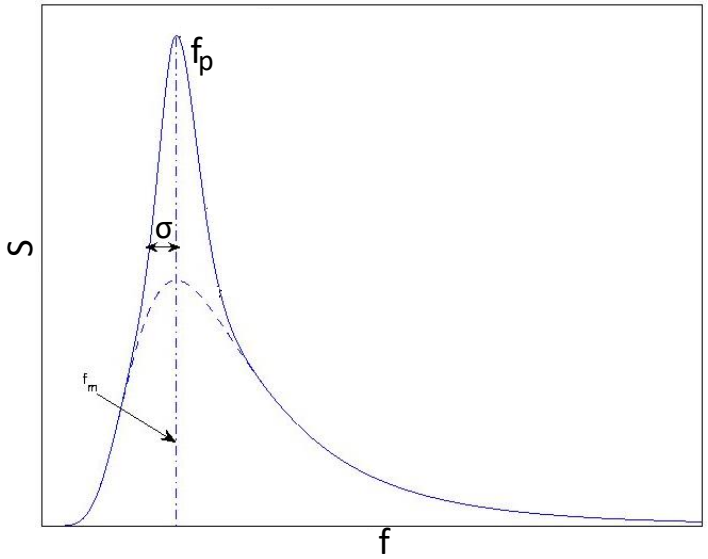

Figure 2.7: Example of a JONSWAP spectrum (wikiwaves.org)

The spectral moments can be employed to compute the spectrum-averaged parameters:

- $H_{m0} = 4m_0$
- $T_{01} = \dfrac{m_0}{m_1}$
- $T_{02} = \sqrt{\dfrac{m_0}{m_2}}$
- $T_{-10} = \dfrac{m_{-1}}{m_0}$
- $T_p = f_p^{-1}$
- $T_c = \sqrt{\dfrac{m_2}{m_4}}$

with $T_p > T_{-10} > T_{01} > T_{02} > T_c$. It can be noticed how much more information on a sea state can be carried out in comparison to the statistical description of sea states.

The model so far discussed applies if all the waves are characterized by the same incoming direction. However, in reality sea waves travel along several different directions, as shown in the example of Figure 2.8.

In view of the above, the complete description of a sea state requires to extend the frequency spectrum over the directions characterizing the propagation of the single waves (referred to as θ_i). Therefore, it is needed to introduce the concept of directional spectrum, which describes the distribution of $S(f)$ with respect to all the possible θ_i. An example of a 2D spectrum can be appreciated in Figure 2.9, while the mathematical formulation is expressed in Equation (2.5) (Goda, 1988).

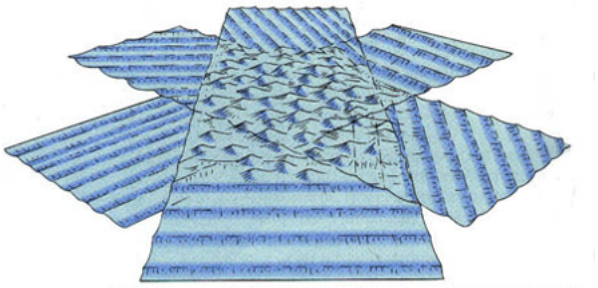

Figure 2.8: Random sea surface due to the superposition of monochromatic waves with different directions

$$S(f,\theta) = S(f)\theta_s(\theta|f) \tag{2.5}$$

where $\theta_s(\theta|f)$ is the so *spreading function*, which controls the directional spreading around the mean wave direction (Kumar et al., 2000).

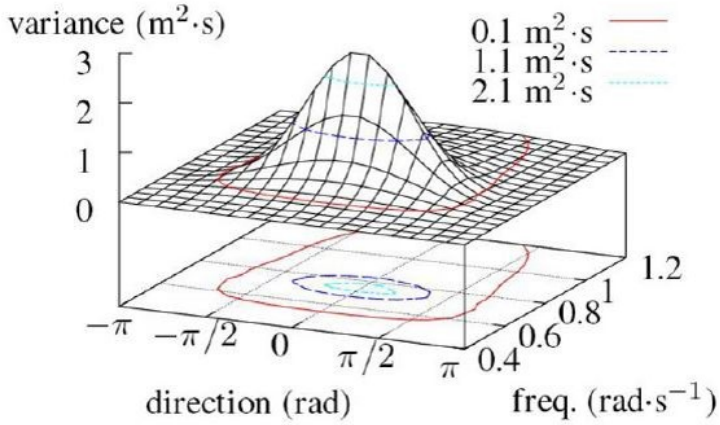

Figure 2.9: Example of a 2D spectra. The wave energy density S depends on f and θ

Once the $S(f,\theta)$ spectrum of a sea state is characterized, the information on respective wave height, period and waves incoming direction can be accordingly inferred. Other parameters that might be of interest, such as wave celerity, wave length etc. can be computed at a second time starting from wave height and period (details can be found in Wood and Fleming, 1981, a.o.).

The sampling of 2D spectra can be carried out through *in-situ* or remote sensing techniques. In this framework, HF-radars undoubtedly worth to be deepened, since they allow to sample wave spectra over wide regions, with the advantage of being installed on the ground. These instruments are commonly employed to sample long-shore currents; as far as wave parameters are concerned, the use of HF-radars has just recently started to be investigated, thus further analysis are required to test the reliability of these devices. Chapter 3 addresses this issue, presenting a study case on the validation of HF-radar wave measures in the Gulf of Naples. However, for the remainder of this work, it is first necessary to define what an *extreme wave* is, and to introduce the theory underlying the analysis of the extremes.

2.2. Extreme Waves

According to Hansom et al. (2015), extreme waves can be grouped in four different categories:

- *Storm waves*: they are commonly produced by very strong winds blowing for lengthy periods and long fetches, resulting in high and long waves that can be amplified by high water levels known as storm surge (Pugh and Woodworth, 2014). They can be observed both in the open ocean and along coastlines, and their height may considerably varies due to local effects and sampling interval;

- *Giant* or *Rogue Waves*: they occur during major storms and they are characterized by steeper forward face preceded by a deep trough or "hole in the sea" (Mallory, 1974). They can arise due to the interaction of different on-phase waves (Rosenthal and Lehner, 2008) and/or to current focusing (White and Fornberg, 1998);

- *Tsunamis*: they are single waves generated by sub-sea earthquakes. They can travel long distances across the oceans at high speed. Although tsunamis are normally not very high in deep water, they can significantly increase when approaching the coastline due to bathymetry effects;

- *Meteotsunamis*: they are atmospherically induced ocean waves that are within the tsunami frequency band (Bryant, 2001).

Extreme waves are fundamental in a number of different ocean and coastal engineering applications, including the design and operation of ships and offshore structures (Vanem, 2015), marine energy generation (Agarwal et al., 2013), aquaculture and coastal installations (Panchang et al., 2008) and coastal vulnerability assessment (De Leo et al., 2019). Indeed, series of extreme H_s (either modeled and/or recorded) are used as key input to calculate the probability of occurrence of hazardous extreme sea states according to the so-called "Extreme Values Theory", which is accordingly introduced in the next Section.

Figure 2.10: Left panel: storm waves approaching the coastline of Genoa (www.ilsecoloxix.it); right panel: rogue wave approaches the Stolt Surf in Oct. 1977 (Photo: Karsten Petersen, www.global-mariner.com)

2.3. The Extreme Values Theory

The Extreme Values Analysis, often referred to as "EVA", play a crucial role for most the engineering projects and designs in the framework of geophysical sciences and applications. The theory at the basis of such analysis, accordingly called Extreme Values Theory (or "EVT"), allows to quantify the probability related to events more extreme than any that have already been observed. Therefore, civil and environmental engineers have always to deal with EVA to account for the likelihood of rare events in nature. As an instance, suppose that a skyscraper with a lifetime of 200 years is meant to be designed at a given site. Among several design requirements that have to be considered, one would be the resilience of the building against the wind blowing over its surface. The easiest way to assess the maximum wind speed the skyscraper will most likely have to face, could be that of evaluating the historical records of the local wind climate. Nevertheless, it is unlikely to have two hundreds years of available data, and even in that case, there is no guarantee that the maximum data occurred in the past will be the upper limit of future wind speeds during the lifetime of the structure. EVA allows to extrapolate the maximum expected wind velocity in a given time frame (two hundreds years in the example). More in general, all the engineering projects and management plans need to account for unpredictable events and the uncertainty characterizing environmental data and processes. In fact, the survival of a given system depends on its capability to withstand the extreme conditions it can be subjected to, and not simply the typical values (Kottegoda and Rosso, 2008).

The EVT aroused starting from the beginning of the last century (e.g. Fisher and Tippett, 1928; Gumbel, 1935), and nowadays is one of the most important statistical disciplines for the applied sciences. EVT is well settled among the scientific community, and applications framed in this theory may be found in many different fields, such as (but not limited to) economy and finance (Gençay and Selçuk, 2004, 2006; Ren and Giles, 2010), medicine and molecular biology (Roberts, 2000; Li and Grosse, 2003), pollutant concentration (Huang and Batterman, 2003; Ercelebi and Toros, 2009), water levels and river discharge (Mudersbach and Jensen, 2010; Yang et al., 2010), met-ocean variables (Goda, 1988; Méndez et al., 2008). Needless to say, the aforementioned list is just a short summary of what can be found in the literature related to this theory.

EVT relies on the assumption that the events under investigation, related to a physical quantity referred to as X, come from a continuous probability distribution with mass function f.

$$f(x) = \Pr(X = x) \tag{2.6}$$

with $x \in R$ and being f the probability that X takes value x. Under this hypothesis, the observations of X are simply particular realizations of the distribution. From now on, X will refer to a variable continuous in the real space. Therefore, if f is known, it is possible to compute the expected realizations related to defined levels of probability.

However, in practice it is often easier to refer to the *probability distribution function*, defined as:

$$F(x) = \Pr(X \leq x) \tag{2.7}$$

Starting from F, it is possible to compute the value of x that is characterized by a given probability of not being exceeded by all possible realizations of X, which is a more reliable assumption, since it is not possible to uniquely assign probabilities to all the values a continuous variable might span (Coles et al., 2001).

$F(x)$ is accordingly referred to as "probability of non-exceedance" of x and is in turn related to the so called *return period* according to the following relation:

$$F(x) = 1 - \frac{1}{\lambda T_r} \tag{2.8}$$

where λ is the yearly number of expected occurrences of x and T_r is the return period, defined as the average time between two successive events characterized by intensity x (Mays, 2010). T_r is widely used, for example, in risk analysis and engineering projects, whose design requires to compute the intensity of forcing related to return periods specified in regulations and recommended practices.

The selection of the extreme data can be performed in three different ways (DNV, 2010):

- retaining the whole starting dataset. This approach is commonly called *global model* or *Initial Distribution* (ID) approach;
- retainig the annual maxima (AM) for the variable under investigation;
- retaining all the exceedances above a given threshold. This approach is referred to as *Peak Over Threshold* or POT approach.

The selection of the data is characterized by a trade-off. When the ID approach is chosen the whole dataset is used, thus the number of points is large (for example in hundreds of thousands for a hindcast covering around 40 years of data) and the uncertainty in the fitting of the distribution is reduced. In this case, the main problem is that the data are highly correlated and this may cause the distribution fitting to be unable to discriminate the tail behavior properly. Moreover, EVT requires the data to be *independent and identically distributed* (the so called iid condition, see Lang et al., 1999, for details). Since the ID dataset violates this condition, some precautions have to be taken for the computation of the high return period values of x, making the ID approach no longer competitive. For AM and POT approaches, where a subset of the whole dataset is used, the iid condition is most likely to be matched, but the scarceness of the data might increase the statistical uncertainty. This makes the POT the preferred approach, since it is not confined to one event per year, leading to a smaller statistical uncertainty. However, the selection of the threshold is critical and still a widely questioned topic (Cavanaugh et al., 2015; Davison and Huser, 2015), thus it should be carefully performed. A sketch representing the selection of data within the POT approach is reported in Figure 2.11. It can be noticed how, even in the framework of the POT data selection, there exist two different approaches. One implies to retain all the exceedances, like those highlighted with the red color in the example (Fawcett and Walshaw, 2007, 2012). Such approach guarantees the availability of huge samples, since there is no need to waste any data, though it requires to modify the computation of the error related to the fitting of the distribution, to consider the serial dependence between the selected data. The other approach implies to perform a de-clustering of the exceedances, i.e. groups of

exceedances are separated due an inter-event duration (often referred to as inter-arrival threshold time, henceforth I_{th}). If the time elapsed between two clusters is higher than I_{th}, the clusters are considered as different events, and the two maximum values of each cluster are retained for further computations (the blue triangles in the example). Otherwise, in case the elapsed time is lower than I_{th}, the clusters belong to the same event, and just the absolute maximum is retained (examples can be found in Claps and Laio, 2003; De Michele et al., 2007; Callaghan et al., 2008, among others). In the latter case, one points will be retained instead of one (the first peak among the two blue triangles in the example).

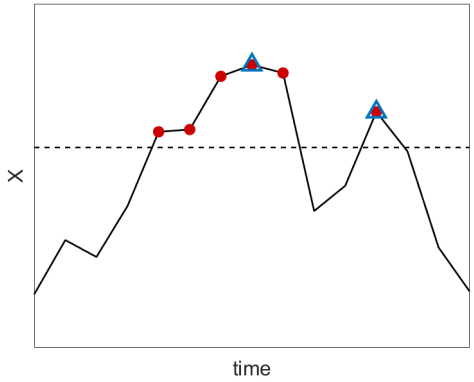

Figure 2.11: Example of a POT data selection. Red circles indicate the exceedances of the threshold, underlined with the black dashed line; blue triangles refer to the peaks of the single clusters

Looking at Equation (2.8), it is evident how the length of the starting dataset directly affects the levels of $F(x)$, since it is reflected on the term λ (i.e. in the average frequency of occurrence of the extreme events). In addition to that, data selection conditions also the probability distribution that shall be tested. For example, if the analysis takes advantage of AM dataset, it is a common practice to rely on the so called Generalized Extreme Value distribution (henceforth GEV, Muraleedharan et al., 2011; Coles et al., 2001; DNV, 2010; Vanem, 2015), whose cumulative distribution function is defined as follows:

$$F(x) = \exp\left[-\left[1+\xi\left(\frac{x-\mu}{\sigma}\right)\right]\right] \tag{2.9}$$

where ξ, μ and σ are the shape, location and scale of the distribution, respectively. Three sub-families of distribution depend on the GEV one. The cases $\xi = 0$, $\xi > 0$ and $\xi < 0$ correspond to the Gumbel (Type I), Fréchet (Type II) and Weibull (Type III) distribution, respectively.

If POT data are employed, a common adopted distribution is instead the Generalized Pareto (henceforth GPD, see Pickands III et al., 1975; Hosking and Wallis, 1987; Castillo and Hadi, 1997):

$$F(x) = 1 - \left[1+\xi\left(\frac{x-\mu}{\sigma}\right)\right]^{-\frac{1}{\xi}} \tag{2.10}$$

according to the notation introduced for the GEV, ξ, μ and σ indicate the shape, location and scale of the distribution, respectively. If the shape ξ and location μ are both zero, then the GPD is equivalent to the exponential distribution.

The aforementioned models arise from the so called *extremal types theorem* for block maxima (in case of GEV) and high threshold exceedances (in case of GPD). However, the mathematical proof leading to the definition of the distribution families is beyond the scope of this summary; interested readers are referred to Coles et al. (2001).

It should be pointed out that GEV and GPD represent just two distributions among many others, and it is not obvious which is the one best fitting the extreme data. Therefore, they shall be used as first attempts to model the study dataset, but it is always recommended to try different distributions, whose efficiency has to be validated either through goodness-of-fit tests (like the Kolmogorov-Smirnov test, see Massey Jr, 1951), and/or through graphical analysis. Figure 2.12 provides an example of the latter case. In the left panel, the empirical quantiles of the X data are compared to those of the real parent distribution; on the right panel, quantiles are compared to those of a distribution that clearly fails to model the data. This analysis takes the name of qq-plot (an abbreviation for "quantile-quatile" plot).

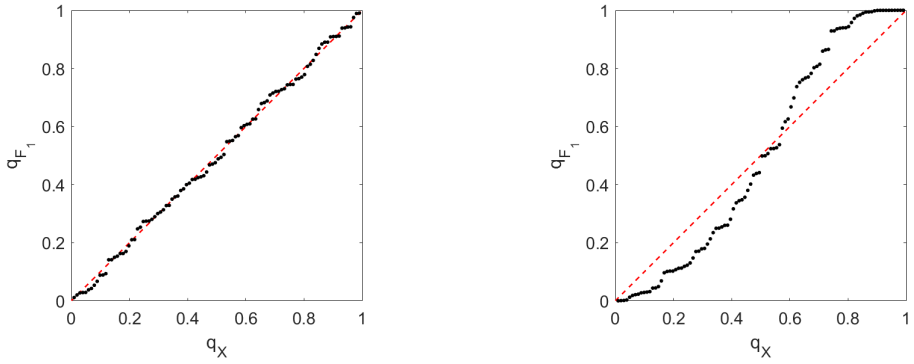

Figure 2.12: Example of a qq-plot for two different distributions

Finally, another distribution that deserves a particular mention is the Poisson frequency distribution (Haight, 1967), whose probability mass function reads:

$$f(k) = \frac{\lambda^k e^{-\lambda}}{k!} \tag{2.11}$$

It refers to the frequency of occurrence of extreme events (instead of their magnitude, as in the case of GEV and GPD). Theoretically, Equation 2.8 holds just if the events under investigation come from a Poisson-point-process, i.e. if the events are randomly located within the overall time window they belong to. Under this assumption, every year has the same probability of providing λ extreme events, being λ the average yearly amount of events identified. Nonetheless, it is worth to mention that the condition on the frequency of occurrence of the data is not as much relevant as the iid condition, since the former has proved not to significantly affect the subsequent EVA (Cunnane, 1979; Önöz and Bayazit, 2001).

As for the fitting of the distribution to the extreme data, commonly used techniques are i) the Method of Moments (MOM or MME), which implies to equal the datasets moments (mean,

variance and skewness) to the moments of the population that depend on the parameters of the selected distribution (Bowman and Shenton, 2014); ii) the Maximum Likelihood Estimation (MLE, see Myung, 2003), which requires to maximize the so called log-likelihood function:

$$L(\theta) = \sum_{i}^{n} \log(f_i(x_i; \theta)) \tag{2.12}$$

where $x_{1:n}$ are independent realizations of a random variable having probability density function $f(x_i; \theta_0)$, being θ_0 the parameters of the distribution.

iii) Last, it is introduced the method of the L-moments, since the research further shown will take advantage of it. L-moments are an alternative system of describing the shapes of probability distributions (Hosking and Wallis, 2005). Analogously to the MOM, this method first requires to compute the moments (in this case the L-moments) of the sample:

$$\begin{cases} l_1 = b_0 \\ l_2 = 2b_1 - b_0 \\ l_3 = 6b_2 - 6b_1 + b_0 \\ l_4 = 20b_3 - 30b_2 + 12b_1 - b_0 \end{cases} \tag{2.13}$$

where b is computed as:

$$b_r = n^{-1} \sum_{j=r+1}^{n} \frac{(j-1)(j-2)\dots(j-r)}{(n-1)(n-2)\dots(n-r)} x_{j:n} \tag{2.14}$$

the moments of Equation 2.13 are then used to estimate the parameters of the selected distribution. Examples of different fitting methods used can be found in Goda (1989) and Mathiesen et al. (1994).

When the parameters, and thus the shape, of the parent distribution are known, it is enough to equal its cumulative distribution function with Equation 2.8, to compute the value of x corresponding to an assigned return period.

In summary, for a given variable of interest (say X), the work-flow of the EVA reads:

1. select the referring extreme events to be modeled through an extreme value distribution
2. select the distribution best modeling the peaks previously identified (the so-called "parent distribution")
3. compute the values of X related to target probabilities and due to its parent distribution

Although the methodology of the EVA seems straightforward, there are still some open issues that worth to be deepen. For example, there is still no consensus on how to properly select the starting dataset of extremes; this is a crucial stage of the analysis, since all the following computations will be strongly affected by the sample of data retained. Furthermore, once the starting set has been chosen, it could be interesting to perform independent EVA on subsets related to particular features of X, though the clustering of X need to comply with statistical hypothesis that complicate the whole procedure. Finally, it is worth to deepen how the possible

time dependency structure of the data affects the EVA. As a matter of fact, the models so far discussed assume stationary conditions for the data but this is not always a reliable condition, for example due to climatic trends driven by global climate change. Usually, a pragmatic approach to embed the intra-period trend in the EVA is that of modeling the distribution parameters as functions of time. This approach has been applied to several different environmental data, such as ocean waves (Vanem, 2015), air temperature (Wang et al., 2013), droughts (Burke et al., 2010) etc. In case of GEV distribution, the three parameters can be defined as:

$$\begin{cases} \mu(t) = \mu_0 + \mu_1 t \\ \sigma(t) = e^{(\sigma_0 + \sigma_1 t)} \\ \xi(t) = \xi_0 + \xi_1 t \end{cases} \tag{2.15}$$

The methodologies used to fit the distributions vary according to the modified relations of the parameters. Please note that the model proposed in Equation 2.15 is just one possible way of explaining the time-dependency of the parameters. To include non-stationarity of the extremes is not trivial, and the time dependency of the variables should be characterized starting from detailed analysis on the starting dataset.

To conclude, it is worth to mention that this Chapter is not intended to exhaustively explain the cornerstone of the EVA. It is meant instead to trace the basis of the EVA that will be used for the researches shown further on the text, where novel methodologies for the analysis of extreme sea states will be developed in the framework of EVT.